AIP Journal of Applied Physics

Effect of bismuth content on the properties of Sr 0.8 Bi x Ta 1.2 Nb 0.9 O 9+y ferroelectric thin films

Huei-Mei Tsai, Pang Lin, and Tseung-Yuen Tseng

Citation: Journal of Applied Physics **85**, 1095 (1999); doi: 10.1063/1.369234
View online: http://dx.doi.org/10.1063/1.369234
View Table of Contents: http://scitation.aip.org/content/aip/journal/jap/85/2?ver=pdfcov
Published by the AIP Publishing

Articles you may be interested in

Degradation and recovery of polarization under synchrotron x rays in Sr Bi 2 Ta 2 O 9 ferroelectric capacitors
J. Appl. Phys. **97**, 044106 (2005); 10.1063/1.1851598

Heat-treatment-induced ferroelectric fatigue of Pt/Sr 1x Bi 2+y Ta 2 O 9 / Pt thin-film capacitors
Appl. Phys. Lett. **81**, 1477 (2002); 10.1063/1.1502010

Improvement in ferroelectric properties of SrBi 2 Ta 2 O 9 thin films with Bi 2 O 3 buffer layers by liquid-delivery metalorganic chemical-vapor deposition
Appl. Phys. Lett. **79**, 1519 (2001); 10.1063/1.1400077

Stress effects of the inter-level dielectric layer on the ferroelectric performance of integrated SrBi 2 Ta 2 O 9 capacitors
J. Appl. Phys. **89**, 8011 (2001); 10.1063/1.1371277

Compositional dependence of electrical characteristics of SrBi 2 (Ta 1x Nb x) 2 O 9 thin-film capacitors
J. Appl. Phys. **84**, 6788 (1998); 10.1063/1.369010

Re-register for Table of Content Alerts

Create a profile.
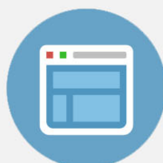
Sign up today!

[This article is copyrighted as indicated in the article. Reuse of AIP content is subject to the terms at: http://scitation.aip.org/termsconditions. Downloaded to] IP: 140.113.38.11 On: Thu, 01 May 2014 08:47:49

JOURNAL OF APPLIED PHYSICS VOLUME 85, NUMBER 2 15 JANUARY 1999

Effect of bismuth content on the properties of $Sr_{0.8}Bi_xTa_{1.2}Nb_{0.9}O_{9+y}$ ferroelectric thin films

Huei-Mei Tsai,[a] Pang Lin,[a] and Tseung-Yuen Tseng[b]
National Chiao-Tung University, Hsinchu, Taiwan, Republic of China

(Received 28 July 1998; accepted for publication 14 October 1998)

This study investigates the effect of bismuth content on the ferroelectric properties of $Sr_{0.8}Bi_xTa_{1.2}Nb_{0.9}O_{9+y}$ (SBTN, x=1.7, 2.0, 2.5, 2.7, 2.9, and 3.2) thin film capacitors. SBTN films are *in situ* grown on Pt/SiO_2/Si substrates by using two-target off-axis radio-frequency magnetron sputtering at a substrate temperature of 600 °C. The films are crystallized with a high (115) diffraction intensity and exhibit a columnar microstructure. Experimental results indicate that the root mean square surface roughness of the film increases with an increase of the bismuth content. In addition, the ferroelectric properties of the films heavily rely on the bismuth content. Moreover, the 440-nm-thick $Sr_{0.8}Bi_{2.5}Ta_{1.2}Nb_{0.9}O_{9+y}$ films exhibit maximum remanent polarization (2Pr) of 52 $\mu C/cm^2$ and minimum coercive field (2Ec) of 28 kV/cm at an applied voltage of 1.5 V. X-ray photoelectron spectral studies reveal that except for Bi^{+3}, no lower valence state bismuth exists in the $Sr_{0.8}Bi_{2.5}Ta_{1.2}Nb_{0.9}O_{9+y}$ film and bismuth substituted in the strontium site still remains in its +3 valence state. © *1999 American Institute of Physics.* [S0021-8979(99)06302-1]

I. INTRODUCTION

Ferroelectric nonvolatile memory devices have received increasing attention from the perspective of the next generation of highly integrated circuits. A conventionally used ferroelectric material is lead zirconate titanate (PZT).[1,2] However, PZT memories with Pt electrodes suffer from fatigue, in which the switchable polarization declines at around 10^8 read/write cycles. Bismuth oxide layered ferroelectric materials based on $SrBi_2Ta_2O_9$ (SBT) or $SrBi_2Nb_2O_9$ (SBN)[3–8] have become increasingly important because the films exhibit no fatigue up to 10^{12} cycles, and have excellent retention characteristics and a low leakage current on Pt electrodes. The general formula for the Bi containing layer-type compounds is $Bi_2A_{n-1}B_nO_{3n+3}$, where A denotes the 12-fold coordinated cation in the perovskite sublattice, B represents the octahedral site and the bismuth forms the rock-salt type interlayer $(Bi_2O_2)^{+2}$ between the perovskite blocks $(A_{n-1}B_nO_{3n+1})$, and n is the number of octahedral layers within the perovskite sublattice of the structure. For the stoichiometric $SrBi_2Ta_2O_9$ ($n=2$) compound, there is one complete perovskite sublattice created by the Ta–O octahedra in which a 12-fold A cation (i.e., Sr) may reside. Osaka *et al.*[9] studied the phase transition process of SBT thin films prepared by chemical liquid deposition. A fluorite phase initially formed at a low temperature and it transforms into bismuth-layer-structure family or a pyrochlore phase ($x<1.2$ $SrBi_xTa_2O_9$) after 750 °C treatment. Although the bismuth content heavily influences remanent polarization (2Pr), particularly when Sr is deficient, formation of the bismuth layer structure is independent of the bismuth content (x =1.6–3.0 for $SrBi_xTa_2O_9$).[10,11] It was considered that Sr deficiency was compensated by excess Bi[12] owing to the fact that the Bi and Sr ionic radii are nearly identical (Sr^{+2}=1.4 Å, Bi^{+3}=1.3 Å). In addition, if the bismuth valence state is +3, maintaining electrical neutrality would lead to some defect formation in the lattice. Therefore, it shifts the Ta position in the perovskite blocks, and gives rise to permanent electric dipoles. When Sr is in stoichiometry, excess bismuth exists in $(Bi_2O_2)^{+2}$ rock salt layer, not in perovskite lattice. Therefore, although its influence on electric dipoles in perovskite blocks is not significant, it facilitates the grain growth. Both changing the perovskite structure and facilitating the grain growth, caused by the excess bismuth, are essential in controlling the ferroelectric properties. Therefore, investigating bismuth content dependence of ferroelectric properties promises means of optimizing the sputtered film preparation process, because the Bi content in the films normally deviates strikingly from that of the target at a high deposition temperature.[13–16] In this work, we employ a two target off-axis magnetron sputter deposition process to prepare SBTN films containing various amounts of bismuth. The microstructure, electrical properties, and x-ray photoelectron spectra of SBTN thin films are thoroughly studied as well.

II. EXPERIMENT

The SBTN films were deposited on a Pt(150 nm)/ SiO_2 (250 nm)/Si(100) substrates by simultaneous magnetron sputtering from two different sintered targets of $Sr_{0.8}Bi_{2.2}Ta_{1.2}Nb_{0.8}O_9$ and Bi_2O_3 with a diameter of 2 in. The targets were prepared by the solid-state reaction process. The radio frequency input for Bi_2O_3 target was fixed at 20 W, and that for the SBTN target was varied from 70 to 120 W. A chamber pressure of 20 mTorr was maintained by a mixture

[a]Also at: Institute of Materials Science and Engineering.
[b]Also at: Department of Electronics Engineering and Institute of Electronics; electronic mail: tseng@cc.nctu.edu.tw

[This article is copyrighted as indicated in the article. Reuse of AIP content is subject to the terms at: http://scitation.aip.org/termsconditions. Downloaded to] IP: 140.113.38.11 On: Thu, 01 May 2014 08:47:49

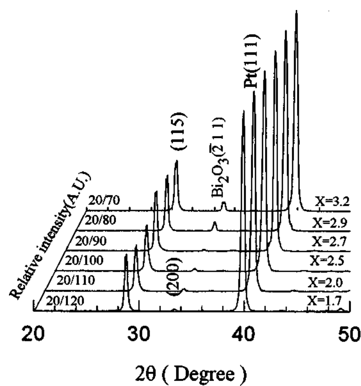

FIG. 1. XRD patterns of 600 °C deposited SBTN films prepared by various radio frequency power ratios.

TABLE I. Chemical composition of 600 °C deposited SBTN films prepared by various radio-frequency power ratios.

Power ratio between Bi_2O_3 and $Sr_{0.8}Bi_{2.2}Ta_{1.2}Nb_{0.8}O_{9+y}$ targets	Mole ratio in SBTN film			
	Sr	Bi	Ta	Nb
20/120W	0.8±0.05	1.7±0.05	1.2±0.05	0.9±0.05
20/110W	0.8±0.05	2.0±0.05	1.2±0.05	0.9±0.05
20/100W	0.8±0.05	2.5±0.05	1.2±0.05	0.9±0.05
20/90W	0.8±0.05	2.7±0.05	1.2±0.05	0.9±0.05
20/80W	0.8±0.05	2.9±0.05	1.2±0.05	0.9±0.05
20/70W	0.8±0.05	3.2±0.05	1.2±0.05	0.9±0.05

of argon and oxygen at a flow-rate ratio of 200/50. Field-emission scanning electron microscopy (FESEM, Hitach S4000) was performed to investigate the surface and cross-sectional morphology of the films. Transmission electron microscopy and energy dispersive spectroscopy (TEM-EDS) examination were performed on a JEOL JEM-2100 which was attached with ISIS 300 energy dispersive x-ray analyzer. The crystal structures of the films were analyzed by using a Siemens D5000 x-ray diffraction (XRD) with Cu$K\alpha$ radiation and a Ni filter. The chemical composition of the films was determined using inductively coupled plasma (ICP) mass spectroscopy (Perkin Elmer, SCIEX ELAN 5000) and secondary ion mass spectroscopy [(SIMS), CAMECA IMS-4f]. Surface roughness of the films was analyzed by using atomic force microscopy [(AFM), NanoscopeIII]. The x-ray photoelectron spectroscopy (XPS) measurements were carried out in a Physical Electronics ESCA PHI 1600 spectrometer at a constant pass energy of 23.5 eV. An Ar^+ ion beam was used to etch the films to obtain the depth profiles of the films. For electrical measurements, Pt top electrodes 1000 Å thick were sputter deposited onto the SBTN films at 300 °C through a shadow mask on an area of 1.77×10^{-4} cm^2. The ferroelectric properties of the films were measured by using a RT66A ferroelectric tester from Radiant Technologies Inc., The current–voltage (I–V) measurements were performed by measuring the current through the sample with a Hewlett–Packard 4145B semiconductor parameter analyzer.

III. RESULTS AND DISCUSSION

XRD studies of SBTN films indicated that the films deposited at temperatures below 500 °C were amorphous and the crystallinity was observed at 600 °C. Figure 1 illustrates the XRD patterns of the films prepared by different power ratios between two targets. According to this figure, all the films reveal a strong (115) reflection, besides that there is a small SBT(200) reflection peak for power ratios lower than 20/90W. As the power ratios exceed more than 20/90W, a Bi_2O_3 peak appears in the XRD pattern. The fact that ferroelectric films are anisotropic accounts for why the crystallographic orientation in ferroelectric materials can heavily influence their properties. According to previous investigations, the crystal orientation more pronouncedly affected the polarization and coercive field values of layer structured SBT and SBN.[17,18] The $(Bi_2O_2)^{-2}$ layer intervening the perovskite-like units along the c axis might not participate in the cooperative phenomenon responsible for ferroelectricity in these materials. The polarization vectors most likely lie close to the a-b plane wherein all the perovskite-like layers are continuous, but do not lie in c axis. Therefore, as expected, our SBTN films [which contain extremely weak (00ℓ) peaks] have larger 2Pr values. The SBTN(115) reflection also exhibited a strong doublet peak ($\Delta 2\theta=0.2°$), which has been described earlier as a strong distortion in the unit cell and a deviation from the actual symmetry.[19]

Table I lists the 600 °C SBTN film compositions obtained from various power ratios. Off-axis sputtering used herein can prevent plasma-bombardment effects and maintain compositional stoichiometry. Table I clearly indicates that the molar numbers of Sr, Ta, and Nb in those films are very close to their target composition, and that the variation of Bi content is attributed to Bi_2O_3 target compensation. However, there still existed a very small compositional difference between the film and target, because we cannot totally eliminate the different sticking coefficients and variation in sputtering yields of the constituent elements.

Figure 2 displays the bismuth SIMS depth profiles of the SBTN films with x=1.7, 2.5, and 3.2. The Bi diffusion through the Pt layer was also observed in this figure. A Bi concentration reaching maximum in the interface of SBTN and Pt bottom electrode implies the formation of Bi_2Pt in the interface. The Bi diffusion was also observed for the SBT films prepared by the sol-gel,[1] metal-organic decomposition

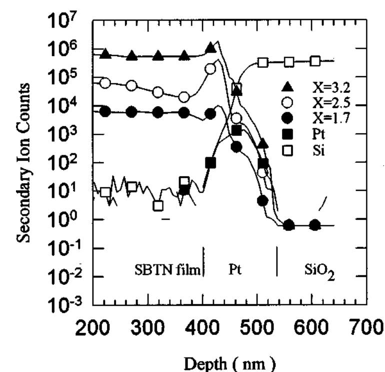

FIG. 2. SIMS bismuth depth profiles of 600 °C deposited $Sr_{0.8}Bi_xTa_{1.2}Nb_{0.9}O_{9+y}$ (x=1.7, 2.5, and 3.2) films.

[This article is copyrighted as indicated in the article. Reuse of AIP content is subject to the terms at: http://scitation.aip.org/termsconditions. Downloaded to] IP: 140.113.38.11 On: Thu, 01 May 2014 08:47:49

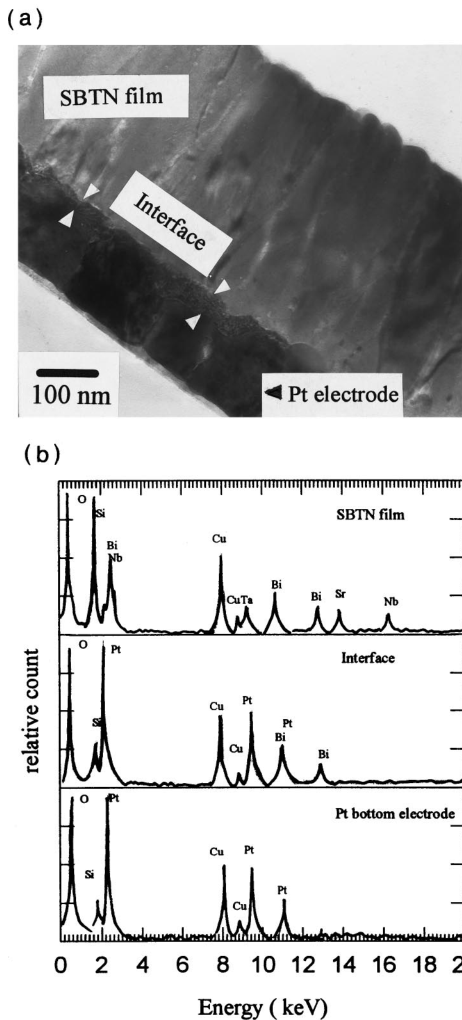

FIG. 3. (a) The cross-sectional TEM image of $Sr_{0.8}Bi_{2.5}Ta_{1.2}Nb_{0.9}O_{9+y}$ film deposited on Pt/SiO_2/Si substrate. (b) EDS spectra acquired from the SBTN, interface, and Pt bottom electrode.

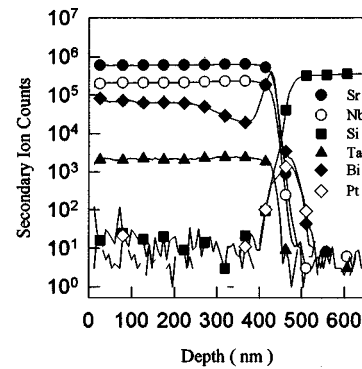

FIG. 4. SIMS depth profiles of $Sr_{0.8}Bi_{2.5}Ta_{1.2}Nb_{0.9}O_{9+y}$ film deposited at 600 °C.

(MOD),[20,21] and metal-organic chemical vapor deposition (MOCVD)[22] techniques. To elucidate the Bi_2Pt formed in the interface, TEM examination was performed. The cross-sectional TEM image of $x=2.5$ SBTN films [Fig. 3(a)] indicates that a layer of 12–40-nm-thick second phase forms at the interface of SBTN film and Pt bottom electrode and the SBTN film had columnar microstructure. The EDS analyses of SBTN, interface, and Pt bottom electrode were made with a 15-nm-diam probe and their spectra are shown in Fig. 3(b). The signals of Cu and Si in Fig. 3(b) come from copper ring and Si substrate during TEM sample preparation using ion gun milling. The major elements at the interface are Bi and Pt. Therefore, the TEM-EDS analysis also reveals that the formation of Bi_xPt second phase in the interface, most probably is Bi_2Pt. As generally recognized, it is extremely difficult for the Bi to get off the bismuth deficiency SBTN film and diffuse into the Pt layer at the deposition temperature of about 600 °C. Hence, according to Fig. 2, the Bi depth profile of $x=1.7$ (i.e., bismuth deficit) film is more uniform than that of $x=2.5$ film. However, for films with $x=3.2$ (i.e., bismuth rich), owing to the presence of Bi_2O_3 phase, evaporation of Bi is expected to be more serious than diffusion. Therefore, there is not significant bismuth depletion region in front of bismuth maximum peak (Fig. 2). The SIMS composition depth profiles of $Sr_{0.8}Bi_{2.5}Ta_{1.2}Nb_{0.9}O_{9+y}$ films (i.e., $x=2.5$ film) indicate that Sr, Ta, and Nb were not diffused into the bottom electrode and their depth profiles are very uniform (Fig. 4). Similar behavior is also found in other films.

Figure 5 illustrates typical (FESEM) surface images obtained from SBTN films having various Bi contents. The films exhibit a somewhat porous structure with elongated grains. The grain size distribution of $x=1.7$ film is nonuniform. In addition, an increase of the bismuth content causes the grain size distribution to become more homogeneous. The average grain size of the $x=2.5$, 2.9, and 3.2 films is about 96 nm. The root means square (rms) roughness of the film surfaces calculated from the AFM morphologies in a 5 $\mu m \times 5$ μm area (Fig. 6) reveals that the roughness of the films increases with an increase of the bismuth content. As generally assumed, increasing Bi content lowers the melting

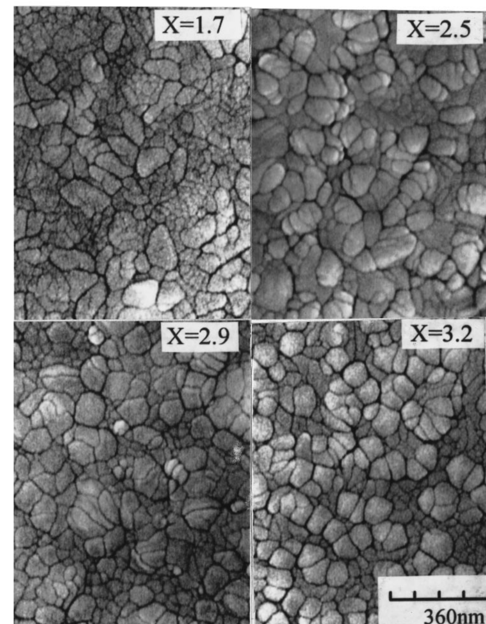

FIG. 5. FESEM surface images of $Sr_{0.8}Bi_xTa_{1.2}Nb_{0.9}O_{9+y}$ ($x=1.7$, 2.5, 2.9, and 3.2) films.

[This article is copyrighted as indicated in the article. Reuse of AIP content is subject to the terms at: http://scitation.aip.org/termsconditions. Downloaded to] IP: 140.113.38.11 On: Thu, 01 May 2014 08:47:49

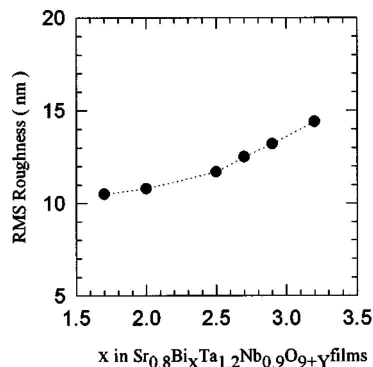

FIG. 6. Root mean square roughness of the various bismuth content SBTN films.

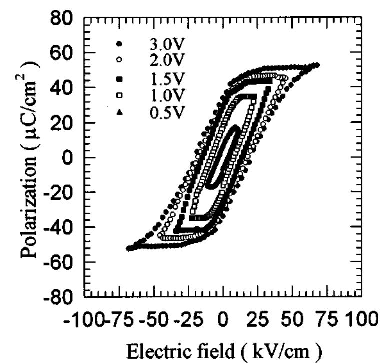

FIG. 8. P–E hysteresis loops of the $Sr_{0.8}Bi_{2.5}Ta_{1.2}Nb_{0.9}O_{9+y}$ films.

point of the films, making it relatively easy to merge small grains into large rough grains during 600 °C deposition.

Figure 7 illustrates the remanent polarization (2Pr) and the coercive field (2Ec) of the different bismuth content SBTN films at an electric field of 35 kV/cm. The SBTN films of $x=2.5$ has a higher remanent polarization than the others, while the coercive fields (2Ec) of the films, except for $x=3.2$, are close to 30 kV/cm. Figure 8 illustrates typical polarization versus electric field curves of $Sr_{0.8}Bi_{2.5}Ta_{1.2}Nb_{0.9}O_{9+y}$ film recorded with -3 to $+3$ V excitations. The 2Pr and 2Ec of $Sr_{0.8}Bi_{2.5}Ta_{1.2}Nb_{0.9}O_{9+y}$ films were 52 μC/cm^2 and 28 kV/cm at an electric field of 35 kV/cm, respectively. These excellent properties may be attributed to the unique solid solution of $SrBi_2Ta_2O_9$ and $SrBi_2Nb_2O_9$ and the crystal orientation control, hence, the Pr value of our SBTN films can be compared with that of PZT. Herein, the fatigue test of the $Sr_{0.8}Bi_{2.5}Ta_{1.2}Nb_{0.9}O_{9+y}$ films was performed using a bipolar square wave of 3 V at 1 MHz, which indicated that no fatigue was observed after the sample was switched up to 1.0×10^{10} cycles. Figure 9 depicts the leakage current densities of the different bismuth content SBTN films at an electric field of 50 kV/cm. The current densities were measured after fabricating the Pt top electrodes followed by annealing in an atmosphere of O_2 at 500 °C for 1 h. According to this figure, the $Sr_{0.8}Bi_{2.5}Ta_{1.2}Nb_{0.9}O_{9+y}$ film exhibits minimum leakage current density of about 1.5×10^{-6} A/cm^2 at an electric field of 50 kV/cm and the Bi deficient films have larger leakage current than the Bi excess films. The leakage current of our films is higher than that of SBT films. The columnar crystallites, the possible Bi_2Pt phase at the interface of SBTN/Pt and the deviation from stoichiometry might be responsible for the higher leakage current density of the SBTN films.

Figure 10 displays the dependence of the Bi signals from XPS of $Sr_{0.8}Bi_{2.5}Ta_{1.2}Nb_{0.9}O_{9+y}$ film on the etching time. The etching rate of the films was 25 nm/min. Obviously, the signal from the film surface is different from that inside. The intensity of the Bi^{+3} signal was high at the film surface and decreased with the etching time, while the intensity of the metallic Bi signal increased with depth. The binding energies of Bi^{+3} $4f_{7/2}$ and $4f_{5/2}$ core level photoemissions were located at 158.8 and 164.2 eV, respectively. The binding energy locations of the metallic bismuth $4f_{7/2}$ and $4f_{5/2}$ core levels, were at 156.4 and 161.8 eV, respectively. After 6 min etching, the amount of metallic Bi was extremely large and there was nearly no trace of Bi^{+3}. These phenomena were attributed to the cleavage of the O–Bi bonds during the Ar ions etching which made bismuth oxide decomposed and reduced to the metallic state.[6,23] Figure 11 illustrates the dependence of the Nb signal from XPS of $Sr_{0.8}Bi_{2.5}Ta_{1.2}Nb_{0.9}O_{9+y}$ film on the etching time. The binding energies of Nb^{+5} $3d_{5/2}$ and $3d_{3/2}$ are 206.6 and 209.4 eV, respectively. After 6 min etching, a signal appeared from metallic Nb, and after 12 min etching, there was no further reduction of Nb^{+5} to Nb. Some of the Bi ions substitute for strontium in its site in $Sr_{0.8}Bi_{2.5}Ta_{1.2}Nb_{0.9}O_{9+y}$ film. XPS

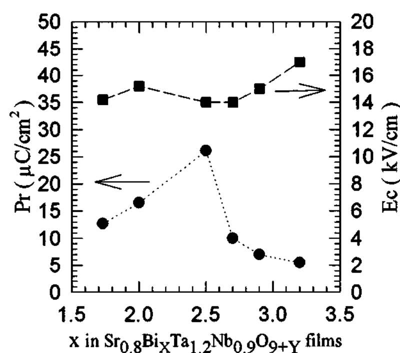

FIG. 7. The remanent polarization and coercive field of the various bismuth content SBTN films at 35 kV/cm electric field.

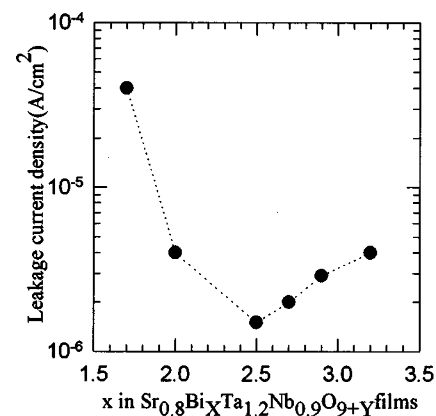

FIG. 9. The current density of the various bismuth content SBTN films at 50 kV/cm electric field.

[This article is copyrighted as indicated in the article. Reuse of AIP content is subject to the terms at: http://scitation.aip.org/termsconditions. Downloaded to] IP: 140.113.38.11 On: Thu, 01 May 2014 08:47:49

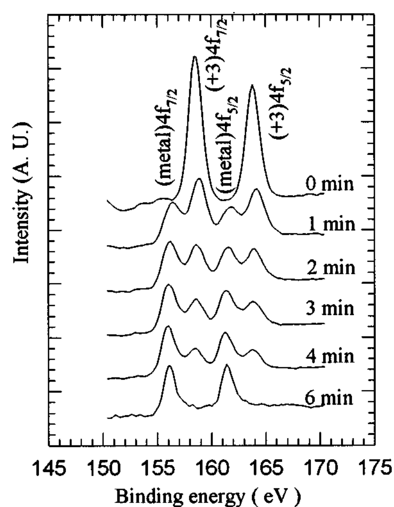

FIG. 10. Etching time dependence of bismuth XPS signals of $Sr_{0.8}Bi_{2.5}Ta_{1.2}Nb_{0.9}O_{9+y}$ film.

studies indicate that there was no lower valence state of bismuth in the film surface except Bi^{+3}. Moreover, metallic Bi in the interior of the film was reduced from Bi^{+3} during argon ion etching. Next, the film after 6 min etching was annealed at 500 °C in O_2 for 1 h and then, the XPS spectrum of this film was recorded at the same spot as before. The metallic Bi and Nb in the interior were observed to be reoxidized to Bi^{+3} and Nb^{+5} states, which are the same as those on the surface of the film. Hence, there was still no lower valence state of bismuth in strontium site. Table II lists the binding energies of this annealed film.

IV. CONCLUSIONS

The bismuth layer structured $Sr_{0.8}Bi_xTa_{1.2}Nb_{0.9}O_{9+y}$ thin films with $x=1.7$, 2.0, 2.5, 2.7, 2.9, and 3.2 were grown on $Pt/SiO_2/Si$ substrates at low temperature of 600 °C by two-target off-axis radio-frequency magnetron sputtering. These films exhibited (115) as the dominant plane and showed co-

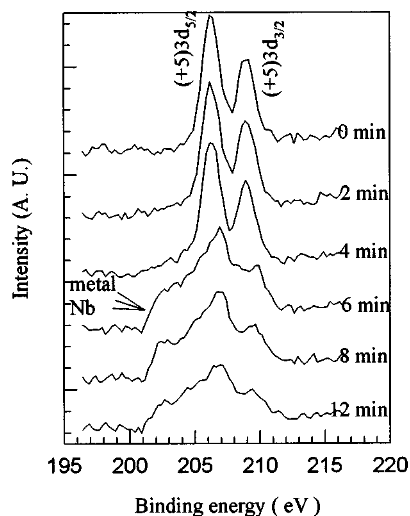

FIG. 11. Etching time dependence of niobium XPS signals of $Sr_{0.8}Bi_{2.5}Ta_{1.2}Nb_{0.9}O_{9+y}$ film.

TABLE II. Binding energy of 600 °C deposited $Sr_{0.8}Bi_{2.5}Ta_{1.2}Nb_{0.9}O_{9+y}$ film.

	Energy level		Valence state	Binding energy (eV)	
Bi	$4f_{7/2}$	$4f_{5/2}$	+3	158.8±0.2	164.2±0.2
Nb	$3d_{5/2}$	$3d_{3/2}$	+5	206.6±0.2	209.4±0.2
Ta	$4f_{7/2}$	$4f_{5/2}$	+5	25.5±0.1	27.3±0.1
Sr	$3d_{5/2}$	$3d_{3/2}$	+2	133.1±0.2	135.6±0.1
O	$1s$		−2	529.6±0.2	

lumnar morphology. When $x \geqslant 2.9$, Bi_2O_3 second phase was found in the film. These films had a low coercive field (2Ec) of about 30 kV/cm at an applied field of 35 kV/cm. In addition, the $Sr_{0.8}Bi_{2.5}Ta_{1.2}Nb_{0.9}O_{9+y}$ film had a larger remanent polarization (2Pr) of 52 μC/cm at 35 kV/cm than other composition films, and also demonstrated fatigue free characteristics up to 1.0×10^{10} switching cycles under a 3 V bipolar 1 MHz square wave. Moreover, XPS depth profiles studies of $Sr_{0.8}Bi_{2.5}Ta_{1.2}Nb_{0.9}O_{9+y}$ film indicated not only that Bi^{+3} and Nb^{+5} appear in both the surface and interior of as-deposited films, but also that bismuth substituted in the strontium site of $x=2.5$ films still remains in its +3 valence state.

ACKNOWLEDGMENT

The author would like to thank the National Science Council of the Republic of China for financially supporting this research under Contract No. NSC 87-2112-M009-037.

[1] T. Y. Tseng, Proceedings of 1996 International Electron Devices and Materials, C2-5, Tsing-Hua University, Hsinchu, Taiwan, 1996, p. 89.
[2] T. Mihara, H. Yoshimori, H. Watanabe, and C. A. Araujo, Jpn. J. Appl. Phys., Part 1 **34**, 5233 (1995).
[3] T. J. Boyle, C. D. Buchheit, M. A. Rodriguez, H. N. Al-Shareef, B. A. Hernandez, B. Scott, and J. W. Ziller, J. Mater. Res. **11**, 2274 (1996).
[4] K. Amanuma, T. Hase, and Y. Miyasaka, Appl. Phys. Lett. **66**, 221 (1995).
[5] P. Y. Chu, R. E. Jones, Jr., P. Zurcher, D. J. Taylor, B. Jiang, S. J. Gillespie, Y. T. Lii, M. Kottke, P. Fejes, and W. Chen, J. Mater. Res. **11**, 1065 (1996).
[6] S. Ono, A. Sakakibara, T. Seki, T. Osaka, I. Koiwa, J. Mita, and T. Iwabuchi, J. Electrochem. Soc. **144**, L185 (1997).
[7] R. Dat, J. K. Lee, O. Auciello, and A. I. Kingon, Appl. Phys. Lett. **67**, 572 (1995).
[8] H. M. Yang, J. S. Luo, and W. T. Lin, J. Mater. Res. **12**, 1145 (1997).
[9] T. Osaka, A. Sakakibara, T. Seki, S. Ono, I. Koiwa, and A. Hashimoto, Jpn. J. Appl. Phys., Part 1 **37**, 597 (1998).
[10] H. Watanabe, T. Mihara, H. Yoshimori, and C. A. Paz de Araujo, Jpn. J. Appl. Phys., Part 1 **34**, 5240 (1995).
[11] T. Atsuki, N. Soyama, T. Yonezawa, and K. Ogi, Jpn. J. Appl. Phys., Part 1 **34**, 5096 (1995).
[12] M. A. Rodriguez, T. J. Boyle, B. A. Hernandez, C. D. Buchheit, and M. O. Eatough, J. Mater. Res. **11**, 2282 (1996).
[13] T. Matsuki, Y. Hayashi, and T. Kunio, Tech. Dig. Int. Electron Devices Meet., 691 (1996).
[14] N. Ichinose and M. Watanabe, Jpn. J. Appl. Phys., Part 1 **36**, 5893 (1997).
[15] S. S. Park, C. H. Yang, S. G. Yoon, J. H. Ahn, and H. G. Kim, J. Electrochem. Soc. **144**, 2855 (1997).
[16] H. M. Tsai, P. Lin, and T. Y. Tseng, Appl. Phys. Lett. **72**, 1787 (1998).
[17] I. Koiwa, T. Kanehara, J. Mita, T. Iwabuchi, T. Osaka, and S. Ono, Jpn. J. Appl. Phys., Part 1 **36**, 1597 (1997).
[18] S. B. Desu, D. P. Vijay, X. Zhang, and B. P. He, Appl. Phys. Lett. **69**, 1719 (1996).
[19] S. B. Desu and D. P. Vijay, Mater. Sci. Eng., B **32**, 75 (1995).

[This article is copyrighted as indicated in the article. Reuse of AIP content is subject to the terms at: http://scitation.aip.org/termsconditions. Downloaded to] IP: 140.113.38.11 On: Thu, 01 May 2014 08:47:49

[20] T. Hayashi, H. Takahashi, and T. Hara, Jpn. J. Appl. Phys., Part 1 **35**, 4952 (1996).
[21] T. Noguchi, T. Hase, and Y. Miyasaka, Jpn. J. Appl. Phys., Part 1 **35**, 4900 (1996).
[22] N. J. Seong, C. H. Yang, W. C. Shin, and S. G. Yoon, Appl. Phys. Lett. **72**, 1374 (1998).
[23] Y. Oishi, Y. Matsumuro, and M. Okuyama, Jpn. J. Appl. Phys., Part 1 **36**, 5896 (1997).

[This article is copyrighted as indicated in the article. Reuse of AIP content is subject to the terms at: http://scitation.aip.org/termsconditions. Downloaded to] IP: 140.113.38.11 On: Thu, 01 May 2014 08:47:49